PHYSICAL REVIEW B **94**, 081102(R) (2016)

# First-principles design of a half-filled flat band of the kagome lattice in two-dimensional metal-organic frameworks

Masahiko G. Yamada,[1,2,*] Tomohiro Soejima,[3] Naoto Tsuji,[4] Daisuke Hirai,[2] Mircea Dincă,[3] and Hideo Aoki[2]
[1]*Institute for Solid State Physics, University of Tokyo, Kashiwa 277-8581, Japan*
[2]*Department of Physics, University of Tokyo, Hongo, Tokyo 113-0033, Japan*
[3]*Department of Chemistry, Massachusetts Institute of Technology, 77 Massachusetts Avenue, Cambridge, Massachusetts 02139, USA*
[4]*RIKEN Center for Emergent Matter Science (CEMS), Wako, Saitama 351-0198, Japan*
(Received 28 October 2015; revised manuscript received 14 July 2016; published 8 August 2016)

We design from first principles a type of two-dimensional metal-organic framework (MOF) using phenalenyl-based ligands to exhibit a half-filled flat band of the kagome lattice, which is one of a family of lattices that show Lieb-Mielke-Tasaki's flat-band ferromagnetism. Among various MOFs, we find that *trans*-Au-THTAP (THTAP=trihydroxytriaminophenalenyl) has such an ideal band structure, where the Fermi energy is adjusted right at the flat band due to unpaired electrons of radical phenalenyl. The spin-orbit coupling opens a band gap giving a nonzero Chern number to the nearly flat band, as confirmed by the presence of the edge states in first-principles calculations and by fitting to the tight-binding model. This is a novel and realistic example of a system in which a nearly flat band is both ferromagnetic *and* topologically nontrivial.

DOI: 10.1103/PhysRevB.94.081102

*Introduction*. The exploration and discovery of new strongly correlated or topologically nontrivial materials drive much of modern condensed-matter physics, yet an experimental design of such materials is still challenging. One class of materials that could greatly extend possibilities of material designing is, in our view, metal-organic frameworks (MOFs). These are crystalline materials composed of metal ions and bridging organic molecules, which have been the subject of numerous investigations in inorganic and materials chemistry [1]. Owing to their typically trivial and localized electronic states, MOFs have not attracted much attention from condensed-matter physicists. However, recent experimental success in fabricating atomically layered two-dimensional (2D) MOFs with kagome lattice structures, initiated by the Nishihara group [2–5], is bridging the gap between condensed-matter physics and chemistry. The Dincă group also succeeded in creating 2D MOFs [6,7]. (Similar 2D MOFs have been fabricated by other groups [8–11].) Some of these new 2D MOFs have been theoretically proposed to become organic $\mathbb{Z}_2$ topological insulators [12–17] or half-metallic ferromagnets [18–21].

The kagome lattice has a virtue of its electronic structure exhibiting a flat band at the highest (or lowest) energy. It has been proven that the tight-binding Hubbard model on the kagome lattice has a nontrivial ground state (far different from the atomic limit) showing itinerant ferromagnetism at arbitrary on-site Coulomb repulsion $U > 0$ when the flat band is half-filled [22]. While several classes of lattices are known to show the flat-band ferromagnetism, as proposed by Lieb, by Mielke, and by Tasaki [23–26], the kagome lattice has an advantage that it is a realistic structure from a synthetic point of view, and does not require fine tuning for hopping parameters to accommodate a flat band [27]. When spin-orbit coupling (SOC) is introduced, the energy gap opens between neighboring bands, and the flat band becomes topologically nontrivial with a nonzero Chern number [28]. Although experimental results on a topological insulator in the bosonic system of the kagome lattice are known [29], the fermionic electron system is more useful for possible applications in electronics and spintronics. It has been discussed that if the nearly flat band with a nonzero Chern number is fractionally filled and is well separated from other bands, the system could be a fractional Chern insulator [28,30,31].

So far, it has been difficult to realize a partially filled flat band in a 2D kagome lattice (i.e., one where the Fermi energy is adjusted to the flat band). Whereas some quasi-one-dimensional (quasi-1D) inorganic systems [32–34] and a quasi-1D organic doped molecular system [35] have been proposed as possible candidates for nearly flat-band ferromagnetism, there is no experimental realization in 2D crystalline systems, as originally proposed by Lieb, Mielke, and Tasaki. Theoretically, Liu *et al.* [36] proposed that an In-based 2D organic nanosheet could possess a topologically nontrivial flat band near the Fermi energy; however, this material still needs additional hole doping to be ferromagnetic. Moreover, it may be difficult to experimentally realize such a 2D structure because the highly covalent bond between indium and carbon would not lead to the formation of crystalline materials.

In this Rapid Communication, we propose 2D MOFs with kagome structures from first principles, where we can show that the flat band of a kagome lattice is indeed expected to be half-filled with the appropriate choice of organic ligand. The essential idea is to use an organic neutral radical called phenalenyl as a building block. In the absence of such an organic radical, hole doping would be necessary as described previously [36,37]. Based on first-principles electronic structure calculations, we discuss that the proposed phenalenyl-based 2D MOF becomes ferromagnetic with the flat band having a nonzero Chern number if SOC is taken into account.

*New 2D metal-organic frameworks*. We employ phenalenyl-based ligands [see $Z = C^{\bullet}$ in Fig. 1(a), where $\bullet$

*m.yamada@issp.u-tokyo.ac.jp

 

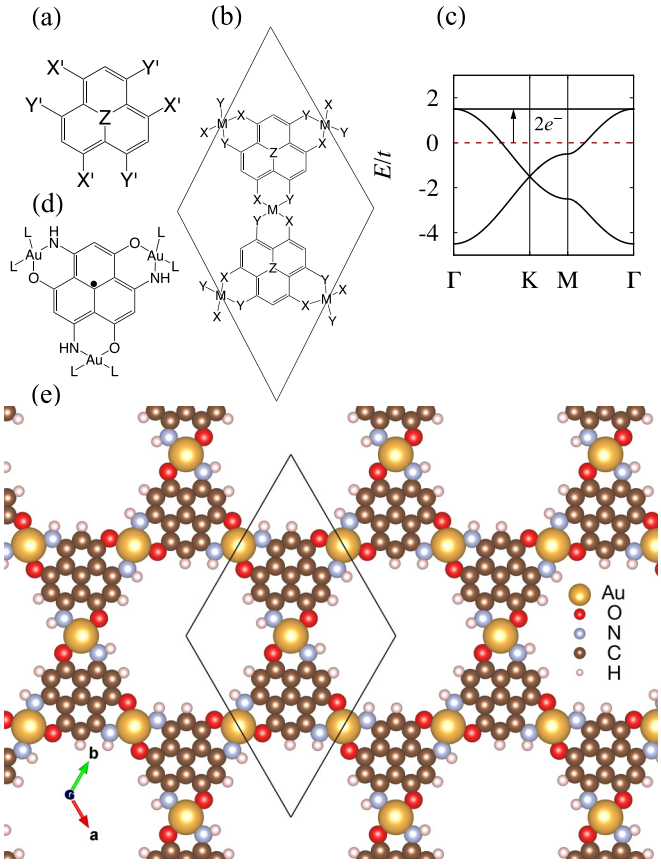


FIG. 1. (a) Molecular structure of the phenalenyl-based ligand ($Z$= C•,N; $X',Y'$= OH, SH, $NH_2$). (b) Structure of the unit cell (solid line) of the proposed MOFs ($M$= Ni, Cu, Pt, Au; $X,Y$= O, S, NH). (c) Band structure of the single-orbital tight-binding model for the kagome lattice with a nearest-neighbor hopping parameter $t$. The brown dashed line shows the Fermi energy when there is one electron per each orbital, while the arrow indicates that the flat band becomes half-filled when two unpaired electrons are transferred from radical phenalenyl. (d) Structure of *trans*-Au-THTAP, where $M$ = Au, $X$ = NH, $Y$ = O, $Z$ = C•, and L stands for a neighboring ligand. (e) Top view of *trans*-Au-THTAP. The solid line indicates a unit cell.

represents an unpaired electron]. Owing to their triangular shape, these exhibit the appropriate symmetry to create kagome structures. These ligands are envisaged to be connected with a transition metal ($M$= Ni, Cu, Pt, Au), where $X$ and $Y$ (=O, S, NH) coordinate [see Fig. 1(b)]. If $M$ is a spin-1/2 metal ($Cu^{2+}$ or $Au^{2+}$ in this case), there is one unpaired electron per orbital on each kagome site [38]. An important advantage of a phenalenyl-based ligand is that we can automatically adjust the Fermi energy from the brown dashed line in Fig. 1(c) to the desired position. This can result in half-filling of the flat band of the kagome lattice by transferring two unpaired electrons per unit cell to $M$ due to the neutral stable radical resonance structure of phenalenyl [see the arrow in Fig. 1(c)]. In the absence of this radical (such as when $Z$= N), electron or hole doping would be necessary, as described previously [16,36,37]. The structure of *trans*-$Au_3(THTAP)_2$ (*trans*-Au-THTAP; THTAP = trihydroxytriaminophenalenyl) [39] with $M$ = Au, $X$ = NH, $Y$ = O is shown in Fig. 1(d). Its whole real-space structure and its unit cell (solid line) are illustrated in Fig. 1(e), with Au atoms occupying each vertex of the kagome lattice.

*Electronic structures from first principles*. The above expectations to realize a half-filled flat band were confirmed from a first-principles electronic structure analysis. To this end, we used the first-principles electronic state calculation code called OPENMX [40], based on density functional theory (DFT). With a repeated slab construction [41], we first calculated possible phenalenyl-based MOFs with $M$= Cu, Au as spin-1/2 ions. In order to conserve a parity symmetry and break other symmetries to lift the degeneracy, we preferred $X \neq Y$ and a *trans*-structure [14,42]. Then, we found that compounds with $M$ = Cu tend to have a bended band, so we focused on $M$ = Au. Finally, we found that all three remaining candidates [with $M$ = Au and $(X,Y)$ = (O, S), (S, NH), (NH, O)] have a nearly flat band exactly lying on the Fermi energy [43]. Among these, *trans*-Au-THTAP [$(X,Y)$ = (NH, O)] has the optimal band structure in the sense that its band structure is accurately matched to that obtained from a tight-binding model on the kagome lattice around the Fermi energy.

*trans-Au-THTAP*. After geometric optimization, *trans*-Au-THTAP was revealed to favor a planar structure [44] with an optimized lattice constant of 16.91 Å. The band structure calculated without SOC is shown in Fig. 2(a). The black solid lines display the spin-up bands, while the blue dashed lines display the spin-down bands. The system shows a metallic nature and the nearly flat band near the Fermi energy [$E$ = 0 in Fig. 2(a)] arising from the kagome lattice is approximately half-filled and indeed spin-polarized. This gives a ferromagnetic behavior with a total spin moment of $1.00\mu_B$/unit cell. We have to note that this spin moment exactly coincides with the expected value for flat-band ferromagnetism [22]. Remarkably, the analysis of the partial density of states (PDOS) for each element clearly shows that the kagome bands near the Fermi energy mostly come from C and N atoms and less from Au $d$ orbitals [see Fig. 2(b)]. This real-space property is further confirmed by the analysis of spin density [45] and could be explained by the itinerant mechanism of ferromagnetism rather than by the interacting localized moments on Au. Moreover, by carrying out a fully relativistic self-consistent calculation on this system, we find that SOC opens a gap of 7.8 meV between the nearly flat band and the lower dispersive band at Γ [compare Fig. 2(c) without SOC to (d) with SOC]. This system has turned out to be still metallic, due to a slight warping of the nearly flat band. The spin-up and spin-down bands are no longer separable when we calculate with SOC, but the $z$ component of the spin ($\sigma^z$) is approximately a conserved quantum number because the calculated magnetic order is always along the $z$ direction in the case of including SOC. This gives a total spin moment of $0.99\mu_B$/unit cell, a total orbital moment of $0.02\mu_B$/unit cell along the $z$ direction, and an exchange splitting of 159.5 meV.

*Topological properties from a tight-binding model*. In order to show the topological nontriviality of the gap between the nearly flat band and the dispersive band of *trans*-Au-THTAP, we first considered a single-orbital tight-binding (TB) model on the kagome lattice, where each single orbital is assumed to be localized around Au. Actually, the wave functions forming the kagome bands are not completely localized on Au and

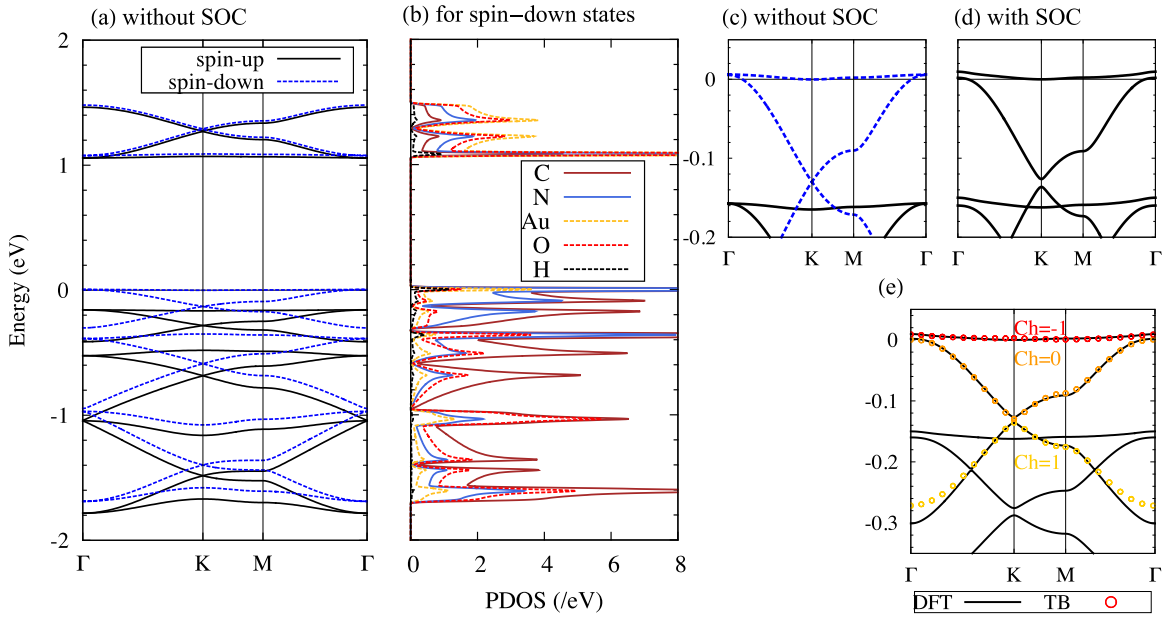


FIG. 2. (a) Band structure of *trans*-Au-THTAP calculated without SOC. The black solid (blue dashed) lines show the spin-up (spin-down) bands. (b) PDOS of the spin-down bands for each element in *trans*-Au-THTAP calculated without SOC. (c) Zoom-in of (a) around the Fermi energy. (d) Zoom-in of the band structure calculated with SOC. (e) Comparison between the band structures calculated with SOC by DFT (solid lines) and by TB (circles) with the calculated Chern numbers (Ch). In each panel, the Fermi energy is taken to be zero.

spreading over the $\pi$-conjugated system, but we can still assume a single-orbital TB model as long as the lattice symmetry is preserved and the parameters of the TB model are somehow renormalized by the effect of spreading. We added a Zeeman term (exchange splitting) to the Hamiltonian considered in [12–14,28,46] to include the effect of ferromagnetism [16]. We considered a complex nearest-neighbor (NN) hopping and a real next-nearest-neighbor (NNN) hopping in a Hamiltonian, $H = E_0 + H_0 + H_{\rm SO} + H_Z$, where

$$H_0 = -t_1 \sum_{\langle ij\rangle\sigma} c^\dagger_{i\sigma} c_{j\sigma} - t_2 \sum_{\langle\langle ij\rangle\rangle\sigma} c^\dagger_{i\sigma} c_{j\sigma}, \tag{1}$$

$$H_{\rm SO} = i\lambda_1 \sum_{\langle ij\rangle\alpha\beta} \nu_{ij} \sigma^z_{\alpha\beta} c^\dagger_{i\alpha} c_{j\beta}, \tag{2}$$

$$H_Z = b \sum_i (-1 - \sigma^z_{\alpha\beta}) c^\dagger_{i\alpha} c_{i\beta}. \tag{3}$$

Here $E_0$ is the energy offset and $c^\dagger_{i\sigma}$ and $c_{i\sigma}$ are the creation and annihilation operators of the $\sigma$-spin electron on the $i$th site of the kagome lattice, respectively. $\langle ij\rangle$ and $\langle\langle ij\rangle\rangle$ denote the NN and NNN bonds, respectively, while $t_1$ and $t_2$ are the corresponding real-valued hopping parameters. $\lambda_1$ is the NN intrinsic spin-orbit coupling and $b$ is the Zeeman splitting, while $\boldsymbol{\sigma}_{\alpha\beta}$ is the Pauli matrix for the spin component. $\nu_{ij}$ is 1 for the counterclockwise hopping and $-1$ for the clockwise hopping when viewed from above. For simplicity, we have omitted the NNN imaginary hopping parameter $\lambda_2$, which is expected to be much smaller than the others [13].

This TB Hamiltonian conserves the $z$ component of the spin, so we can divide the one-particle Hilbert space $\mathcal{H}$ into $\mathcal{H}_\uparrow \oplus \mathcal{H}_\downarrow$ by the eigenvalue of $\sigma^z$. We only consider the space $\mathcal{H}_\downarrow$ because there are only spin-down bands near the Fermi energy. In other words, we have projected out the spin-up states by taking the limit $b \to \infty$ first. We can then accurately fit the kagome bands in the DFT calculation with SOC (solid line) to that obtained from the TB model (circles) around the Fermi energy as shown in Fig. 2(e) with the parameters $E_0 = -87.4$ meV, $t_1 = 45.1$ meV, $t_2 = 1.0$ meV, and $\lambda_1 = 1.2$ meV. Based on the TB model, we can calculate a topological Chern number (Ch) for each band [47,48]. From the results displayed in Fig. 2(e), we can conclude that the nearly flat band is indeed topologically nontrivial with a Chern number of $-1$ within this TB framework.

*Edge states*. Because the topological property of the SOC gap is model dependent, the choice of the SOC term in the TB model can be somewhat arbitrary. A clear way to show the topological nontriviality of the system is to detect the topological edge states by a DFT calculation. To do so, we again used OPENMX with a repeated ribbon construction [49]. The calculated band structure is shown in Fig. 3, where the red and blue dashed lines clearly show the chiral edge states for each boundary and cannot be gapped away. Since we took a different boundary condition for each edge (one with Au aligning along the boundary and the other without Au), they are asymmetric against $k_x = 0$. These edge modes are similar to the ones in Ref. [14] except for the spin polarization due to its ferromagnetism. The emergence of these nontrivial states localized along the boundaries [50] again confirms the topological nature of the nearly flat band. These two results from TB and DFT show that there exists an exotic phase—a topologically nontrivial nearly flat band with full spin polarization.

*Phonon calculations*. To verify the stability of the proposed geometric structure, we also performed phonon calculations.

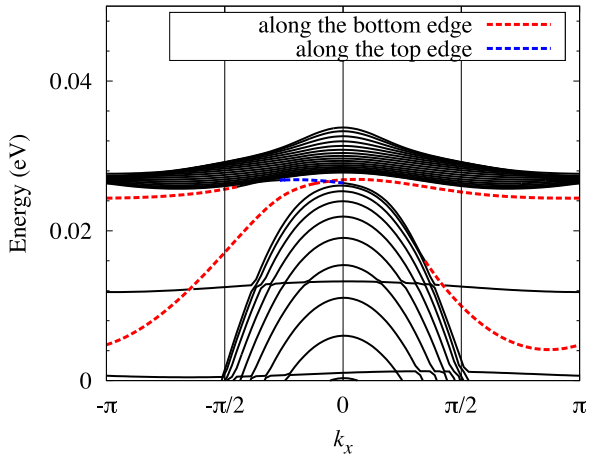


FIG. 3. Band structure for a ribbon of *trans*-Au-THTAP. The black solid lines represent the bulk states, and the red (blue) dashed lines represent topological edge states along the bottom (top) edge.

We used the first-principles electronic state calculation code called QUANTUM ESPRESSO [51]. These studies show that a flat, freestanding sheet of *trans*-Au-THTAP may buckle at low temperature [52], giving rise to imaginary out-of-plane phonon modes (see Fig. S5 in the Supplemental Material). Experimentally, however, sheets of the target material would likely be tested on a flat surface, not freestanding. Thus, we expect that the out-of-plane modes may be suppressed under experimental conditions, thereby retaining the nontrivial properties. Proximity effects, such as Rashba-type SOC, from various substrates on the electronic and magnetic structure of this material could itself make the subject of interesting future theoretical studies.

*Conclusion*. We have proposed several 2D MOFs, and found that *trans*-Au-THTAP has a topologically nontrivial nearly flat band from the DFT calculations. This is a novel and realistic example of a system in which a nearly flat band at the Fermi energy is both ferromagnetic *and* topologically nontrivial. From a synthetic standpoint, we have to note that Au indeed prefers a square planar coordination environment in the +2 formal oxidation state, as discussed in Ref. [53]. We also note that there would be electron correlation effects for the flat-band ferromagnetic ground state that are not properly captured within the DFT framework, which is worthwhile to study in the future.

Although the proposed system does not have a quantized Hall current due to its metallicity, a topologically nontrivial phase realized in the proposed material (called a Chern metallic phase in Ref. [54]) is still worth investigating. At this moment we have only confirmed the existence of the edge states with a constraint on the spin structure. Future work will probe whether magnetic order can exist along the boundaries and how it would affect the topological edge states. Furthermore, it would be interesting to explore whether one could enhance the band gap given the known tunability of MOFs. This would create a ferromagnetic insulator with a quantized Hall conductance (quantum anomalous Hall effect [55]) or a fractional Chern insulator [28,30,31,56–60] with a large (band gap)/(bandwidth) ratio. We note, in this sense, that a no-go theorem has been proven mathematically for topologically nontrivial perfectly flat bands within local tight-binding models [61].

*Acknowledgments*. We wish to acknowledge H. Nishihara, R. Sakamoto, and N. Shima for illuminating discussions in the early stage of the present work, and M. Oshikawa, S. Kasamatsu, M. Kawamura, S. Tsuneyuki, G. Jackeli, H. Takagi, T. Ozaki, R. Osawa, A. Pulkin, and Y. Murotani for helpful comments. This work was supported by JSPS KAKENHI Grants No. JP26247064, No. JP25107005, No. JP25610101, and was funded by ImPACT Program of Council for Science, Technology and Innovation (Cabinet Office, Government of Japan). M.G.Y. is supported by the Materials Education program for the future leaders in Research, Industry, and Technology (MERIT). N.T. is supported by JSPS KAKENHI Grants No. JP25104709 and No. JP25800192. M.D. is supported by the Center for Excitonics, an Energy Frontier Research Center funded by the U.S. Department of Energy, Office of Science, Office of Basic Energy Sciences under award No. DE-SC0001088 (MIT), and by nontenured faculty awards from the Sloan Foundation, the Research Corporation for Science Advancement (Cottrell Scholars), and 3M. The computation in this work has been done with the facilities of the Supercomputer Center, the Institute for Solid State Physics, the University of Tokyo. The initial crystal structures for the geometry optimization have been taken from the Cambridge Crystallographic Data Centre.

[1] MOF is defined as a coordination compound continuously extending in one, two, or three dimensions through coordination bonds with an open framework containing potential voids by IUPAC. See S. R. Batten, N. R. Champness, X.-M. Chen, J. Garcia-Martinez, S. Kitagawa, L. Öhrström, M. O'Keeffe, M. P. Suh, and J. Reedijk, Pure Appl. Chem. **85**, 1715 (2013).

[2] T. Kambe, R. Sakamoto, K. Hoshiko, K. Takada, J.-H. Ryu, S. Sasaki, J. Kim, K. Nakazato, M. Takata, and H. Nishihara, J. Am. Chem. Soc. **135**, 2462 (2013).

[3] T. Kambe, R. Sakamoto, T. Kusamoto, T. Pal, N. Fukui, T. Shimojima, Z. Wang, T. Hirahara, K. Ishizaka, S. Hasegawa, F. Liu, and H. Nishihara, J. Am. Chem. Soc. **136**, 14357 (2014).

[4] R. Sakamoto, K. Hoshiko, Q. Liu, T. Yagi, T. Nagayama, S. Kusaka, M. Tsuchiya, Y. Kitagawa, W.-Y. Wong, and H. Nishihara, Nat. Commun. **6**, 6713 (2015).

[5] R. Dong, M. Pfeffermann, H. Liang, Z. Zheng, X. Zhu, J. Zhang, and X. Feng, Angew. Chem., Int. Ed. **54**, 12058 (2015).

[6] D. Sheberla, L. Sun, M. A. Blood-Forsythe, S. Er, C. R. Wade, C. K. Brozek, A. Aspuru-Guzik, and M. Dincă, J. Am. Chem. Soc. **136**, 8859 (2014).

[7] M. G. Campbell, D. Sheberla, S. F. Liu, T. M. Swager, and M. Dincă, Angew. Chem., Int. Ed. **54**, 4349 (2015).

[8] Z. Shi, J. Liu, T. Lin, F. Xia, P. N. Liu, and N. Lin, J. Am. Chem. Soc. **133**, 6150 (2011).

[9] M. Hmadeh, Z. Lu, Z. Liu, F. Gándara, H. Furukawa, S. Wan, V. Augustyn, R. Chang, L. Liao, F. Zhou, E. Perre, V. Ozolins, K. Suenaga, X. Duan, B. Dunn, Y. Yamamto, O. Terasaki, and O. M. Yaghi, Chem. Mater. **24**, 3511 (2012).
[10] J. Cui and Z. Xu, Chem. Commun. **50**, 3986 (2014).
[11] X. Huang, P. Sheng, Z. Tu, F. Zhang, J. Wang, H. Geng, Y. Zou, C.-a. Di, Y. Yi, Y. Sun, W. Xu, and D. Zhu, Nat. Commun. **6**, 7408 (2015).
[12] Z. F. Wang, N. Su, and F. Liu, Nano Lett. **13**, 2842 (2013).
[13] B. Zhao, J. Zhang, W. Feng, Y. Yao, and Z. Yang, Phys. Rev. B **90**, 201403 (2014).
[14] Q. Zhou, J. Wang, T. S. Chwee, G. Wu, X. Wang, Q. Ye, J. Xu, and S.-W. Yang, Nanoscale **7**, 727 (2015).
[15] S. Chen, J. Dai, and X. C. Zeng, Phys. Chem. Chem. Phys. **17**, 5954 (2015).
[16] X. Zhang, Z. Wang, M. Zhao, and F. Liu, Phys. Rev. B **93**, 165401 (2016).
[17] L. Dong, Y. Kim, D. Er, A. M. Rappe, and V. B. Shenoy, Phys. Rev. Lett. **116**, 096601 (2016).
[18] M. Zhao, A. Wang, and X. Zhang, Nanoscale **5**, 10404 (2013).
[19] H. Hu, Z. Wang, and F. Liu, Nanoscale Res. Lett. **9**, 690 (2014).
[20] J. Liu and Q. Sun, ChemPhysChem **16**, 614 (2015).
[21] X. Zhang and M. Zhao, Sci. Rep. **5**, 14098 (2015).
[22] A. Mielke, J. Phys. A: Math. Gen. **24**, L73 (1991).
[23] E. H. Lieb, Phys. Rev. Lett. **62**, 1201 (1989).
[24] H. Tasaki, Phys. Rev. Lett. **69**, 1608 (1992).
[25] H. Tasaki, Prog. Theor. Phys. **99**, 489 (1998).
[26] H. Aoki, Int. J. Mod. Phys. B **17**, 4953 (2003).
[27] Some honeycomb superlattice structures are also shown to have flat bands. See N. Shima and H. Aoki, Phys. Rev. Lett. **71**, 4389 (1993).
[28] E. Tang, J.-W. Mei, and X.-G. Wen, Phys. Rev. Lett. **106**, 236802 (2011).
[29] R. Chisnell, J. S. Helton, D. E. Freedman, D. K. Singh, R. I. Bewley, D. G. Nocera, and Y. S. Lee, Phys. Rev. Lett. **115**, 147201 (2015).
[30] T. Neupert, L. Santos, C. Chamon, and C. Mudry, Phys. Rev. Lett. **106**, 236804 (2011).
[31] K. Sun, Z. Gu, H. Katsura, and S. Das Sarma, Phys. Rev. Lett. **106**, 236803 (2011).
[32] F. Mizuno, H. Masuda, I. Hirabayashi, S. Tanaka, M. Hasegawa, and U. Mizutani, Nature (London) **345**, 788 (1990).
[33] H. N. Kono and Y. Kuramoto, J. Phys. Soc. Jpn. **75**, 084706 (2006).
[34] R. Arita, Y. Suwa, K. Kuroki, and H. Aoki, Phys. Rev. Lett. **88**, 127202 (2002).
[35] M. Garnica, D. Stradi, S. Barja, F. Calleja, C. Díaz, M. Alcamí, N. Martín, A. L. Vázquez de Parga, F. Martín, and R. Miranda, Nat. Phys. **9**, 368 (2013).
[36] Z. Liu, Z.-F. Wang, J.-W. Mei, Y.-S. Wu, and F. Liu, Phys. Rev. Lett. **110**, 106804 (2013).
[37] Z. Liu, F. Liu, and Y.-S. Wu, Chin. Phys. B **23**, 077308 (2014).
[38] Here $M$ = Ag is excluded since a homologous element Ag is known to have a tendency to form straight complexes.
[39] An IUPAC name for the ligand is 3,6,9-triamino-phenalene-1,4,7-triol.
[40] See http://www.openmx-square.org/.
[41] See Supplemental Material at http://link.aps.org/supplemental/10.1103/PhysRevB.94.081102 for the definition of the repeated slab construction.
[42] A *cis*-structure will break the structure's parity symmetry.
[43] See Supplemental Material at http://link.aps.org/supplemental/10.1103/PhysRevB.94.081102 for all the calculated band structures.
[44] See Supplemental Material at http://link.aps.org/supplemental/10.1103/PhysRevB.94.081102 for the cif files for the relaxed atomic structures.
[45] See Supplemental Material at http://link.aps.org/supplemental/10.1103/PhysRevB.94.081102 for the real-space spin density and Bloch functions.
[46] H.-M. Guo and M. Franz, Phys. Rev. B **80**, 113102 (2009).
[47] T. Fukui, Y. Hatsugai, and H. Suzuki, J. Phys. Soc. Jpn. **74**, 1674 (2005).
[48] Y. Hatsugai, T. Fukui, and H. Aoki, Phys. Rev. B **74**, 205414 (2006).
[49] See Supplemental Material at http://link.aps.org/supplemental/10.1103/PhysRevB.94.081102 for the definition of the repeated ribbon construction.
[50] See Supplemental Material at http://link.aps.org/supplemental/10.1103/PhysRevB.94.081102 for the real-space nontrivial properties of the edge states.
[51] P. Giannozzi *et al.*, J. Phys.: Condens. Matter **21**, 395502 (2009).
[52] See Supplemental Material at http://link.aps.org/supplemental/10.1103/PhysRevB.94.081102 for the phonon dispersion.
[53] A. Laguna and M. Laguna, Coord. Chem. Rev. **193-195**, 837 (1999).
[54] X. Hu, Z. Zhong, and G. A. Fiete, Sci. Rep. **5**, 11702 (2015).
[55] C.-Z. Chang *et al.*, Science **340**, 167 (2013).
[56] E. J. Bergholtz and Z. Liu, Int. J. Mod. Phys. B **27**, 1330017 (2013).
[57] N. Regnault and B. A. Bernevig, Phys. Rev. X **1**, 021014 (2011).
[58] X.-L. Qi, Phys. Rev. Lett. **107**, 126803 (2011).
[59] J. Maciejko and G. A. Fiete, Nat. Phys. **11**, 385 (2015).
[60] D. N. Sheng, Z. C. Gu, K. Sun, and L. Sheng, Nat. Commun. **2**, 389 (2011).
[61] L. Chen, T. Mazaheri, A. Seidel, and X. Tang, J. Phys. A: Math. Theor. **47**, 152001 (2014).